A Synthetic-Geometry, MLC-Aware Machine Learning Framework for Collimator Angle Selection in Single-Isocenter Multi-Target VMAT SRS

Theodore H. Arsenault, MS, Kai-Cheng Chuang, PhD, Prashant Vempati, MD, Haley K Perlow MD, Attallah Baydoun, MD, Rojano Kashani, PhD
University Hospitals Seidman Cancer Center, Cleveland OH

ABSTRACT

PURPOSE:
Collimator orientation in single-isocenter multi-target (SIMT) SRS strongly affects MLC modulation and plan quality. We developed a machine-learning framework to identify optimal collimator angles prior to TPS optimization, minimizing iterative planning and improving deliverability.

METHODS:
500 synthetic SIMT cases (3–10 targets) were generated. Candidate collimator angles were scored from beam's-eye-view (BEV) geometry — island count, small-island fraction, aperture area, perimeter-to-area, and leaf-span statistics — with BEV masks read against HD120 leaf-pair rows. A gradient-boosted tree was trained to predict this composite "source" score (75/25 GroupShuffleSplit by case ID).

RESULTS:
On the held-out test set: MAE 0.381, R^2 0.998, mean regret 0.022. The optimal collimator angle fell within the top-1 prediction in 86.8% of cases and within the top-5 in 99.4%.

CONCLUSION:
This MLC-aware framework enables accurate, pre-optimization collimator selection — standardizing workflows and improving delivery efficiency in SIMT VMAT SRS.

CONTACT
Theodore H. Arsenault, MS
UH Seidman Cancer Center
theodore.arsenault@uhhospitals.org

INTRODUCTION

Single-isocenter multi-target (SIMT) VMAT SRS treats multiple intracranial lesions efficiently from one isocenter. When two or more targets share the same MLC leaf pair, "island blocking" exposes normal tissue between lesions that the leaves cannot shield.

Collimator angle governs how targets project onto the leaf pairs, so it directly controls island formation and MLC modulation burden. Optimal angles are conventionally found by planner heuristics or costly post-optimization complexity metrics — both slow and variable.

We ask the geometry directly: can a model trained on physically interpretable BEV surrogates of MLC modulation rank candidate collimator angles before any TPS optimization runs?

METHODS

Synthetic dataset
Synthetic SIMT cases with 3–10 spherical and ellipsoidal targets at varied spatial distributions, swept over candidate collimator angles on a clinical four-arc template (couch 0°, 315°, 45°, 90°).

BEV geometry → "source" score
For each angle/arc, targets are projected into the BEV at 25 sampled gantry angles and read against HD120 leaf-pair rows. Six metrics are averaged over the gantry samples and combined (lower = better):

- 3.5 × mean island count
- 2.5 × small-island pixel fraction
- mean leaf-span std ÷ 8
- 2.0 × leaf-gap fraction
- 0.8 × perimeter-to-area ratio
- 0.3 × normalized BEV aperture area

Model & validation
A HistGradientBoostingRegressor predicts this score from 32 features (case geometry, arc, angle encoding, and the six BEV metrics). Data were split 75/25 by case ID with GroupShuffleSplit to prevent leakage.

INNOVATION & IMPACT

Unlike approaches that rely on planner heuristics or post-optimization complexity metrics, this method folds BEV target geometry, MLC characteristics, and arc-specific information into a supervised framework that ranks candidate collimator orientations before plan optimization.

The source complexity score is built from physically interpretable BEV surrogates — island aperture formation, leaf-span variability, and perimeter-based complexity — that explicitly approximate MLC modulation burden.

The result is an interpretable, computationally efficient decision-support tool that can reduce planning variability, improve deliverability, and streamline SIMT SRS workflows. Visual QA outputs further support clinical trust and transparency.

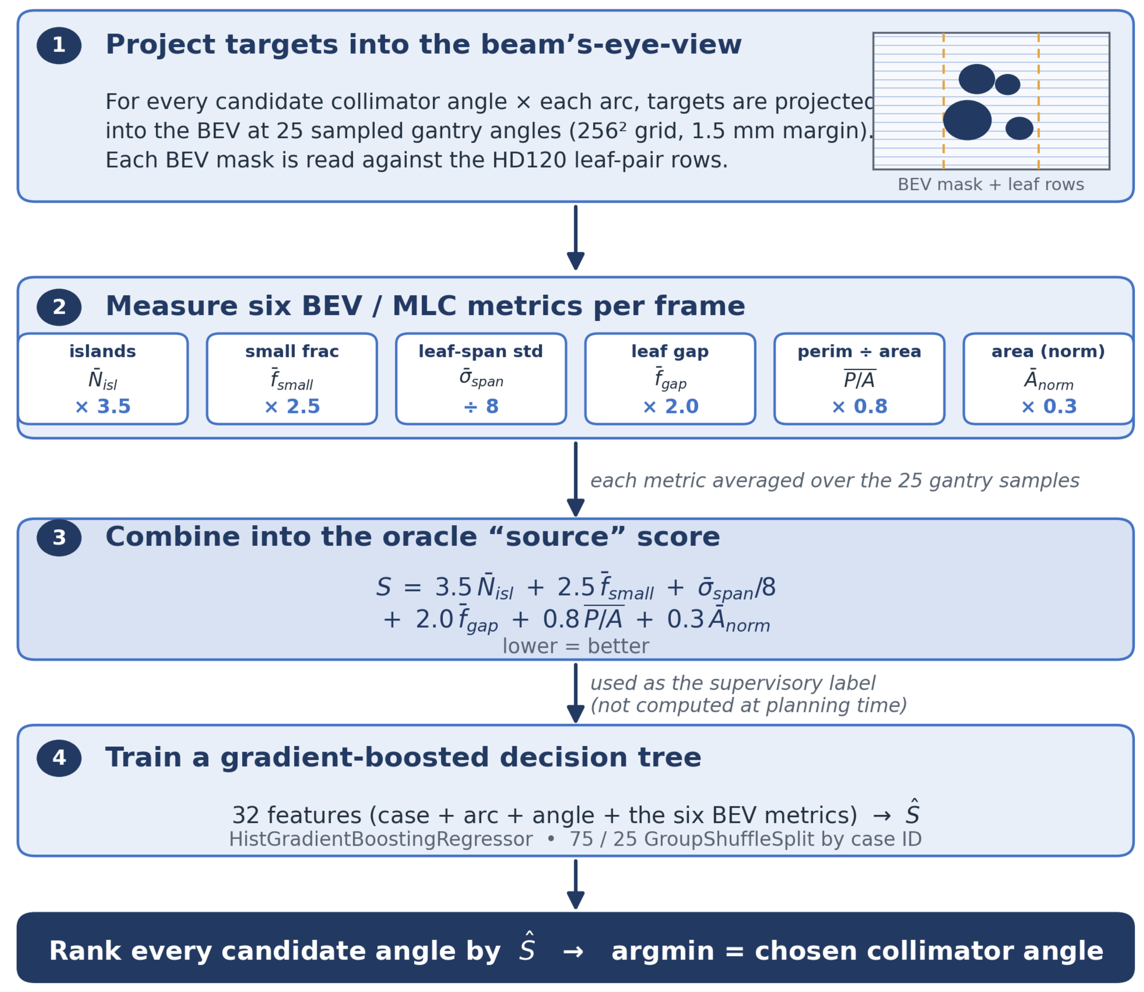

Figure 1. How the predicted score is calculated: BEV geometry → six weighted metrics → oracle score S → GBDT → predicted score for every candidate angle.

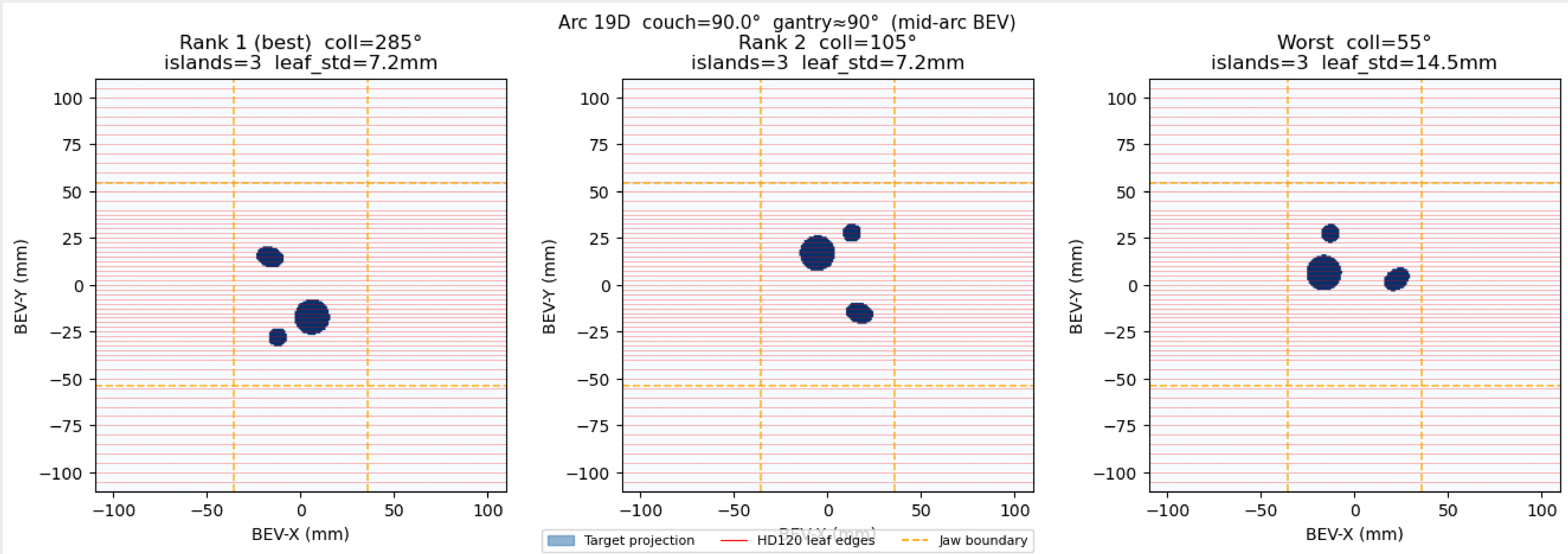

Figure 2. Mid-arc BEV for arc 19D at the rank-1, rank-2, and worst collimator angles. All three leave 3 islands, but leaf-span std rises from 7.2 mm to 14.5 mm at the worst angle — the modulation burden the score captures.

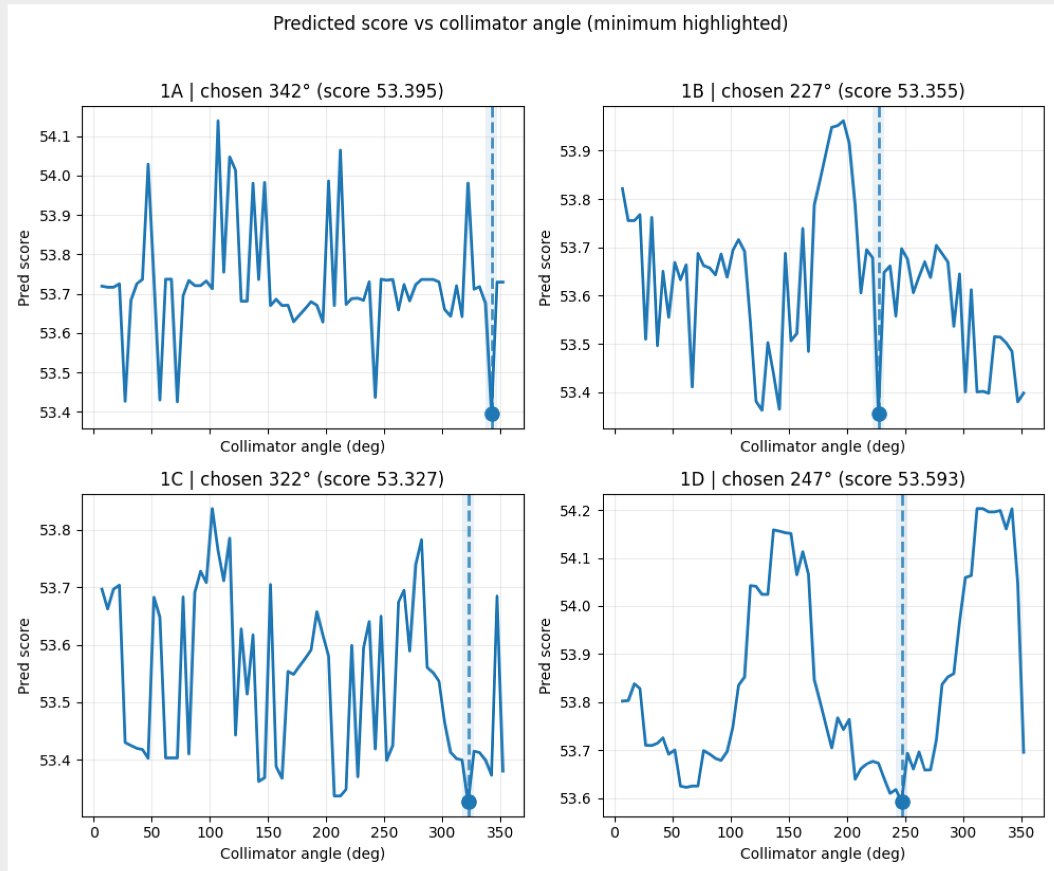

Figure 3. Predicted score vs. collimator angle for four cases; the chosen minimum (dashed) tracks the true optimum.

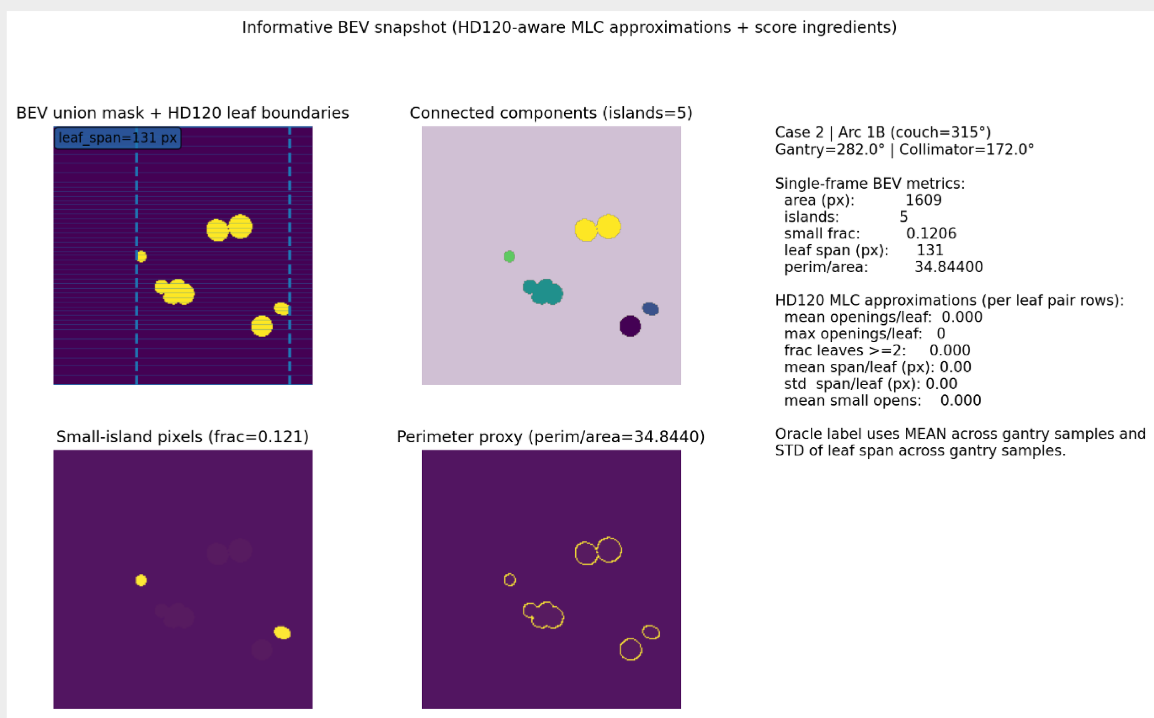

Figure 4. Interpretable BEV / HD120 snapshot on a real case — the score ingredients of Figure 1, shown as visual QA.

RESULTS AND DISCUSSION

On the independent test set the model reproduced the geometry-based oracle score almost exactly:

- MAE = 0.381 • R^2 = 0.998
- Mean regret = 0.022 (score gap vs. true optimum)
- Optimal angle in top-1 prediction: 86.8%
- Optimal angle in top-5 predictions: 99.4%

Near-zero regret means that even when the exact best angle is missed, the predicted angle is effectively equivalent. The model bypasses high-island geometries and hands the TPS optimizer a pre-narrowed search space.

Because the labels are physically interpretable BEV surrogates rather than opaque post-optimization plan metrics, the ranking is transparent and machine-specific — the visual QA panels below let a planner see why an angle was chosen.

CONCLUSION

A gradient-boosted, MLC-aware model predicts optimal collimator angles directly from BEV geometry—before any TPS optimization—with R^2 = 0.998 and the optimum inside its top-5 in 99.4% of cases.

Integrated pre-planning collimator selection can standardize SIMT SRS workflows, cut planning iterations, and improve delivery efficiency. Future work: validation on clinical plans and extension to non-coplanar arc-specific weighting.

REFERENCES

1. Kang J, et al. A method for optimizing collimator angles in single-isocenter multi-target VMAT SRS to reduce island blocking. J Appl Clin Med Phys. 2019.
2. Pudsey L, et al. Collimator angle optimization and jaw tracking for VMAT single-isocenter multi-target SRS in Eclipse. J Appl Clin Med Phys. 2021;22:171-182.
3. Wu Q, et al. Sub-arc collimator angle optimization from a conformity-index heatmap for VMAT SRS of multiple brain metastases. Front Oncol. 2022;12:987971.